GCA-TR-70-5-N

TECHNIQUES APPLICABLE TO MASS SPECTROMETRY OF GASEOUS TRACE CONTAMINANTS

P. Warneck

Bedford, Massachusetts

FINAL REPORT
CONTRACT NO. NAS12-641

PREPARED FOR
NATIONAL AERONAUTICS AND SPACE ADMINISTRATION
ELECTRONICS RESEARCH CENTER
Cambridge, Massachusetts

June 1970

GCA-TR-70-5-N

TECHNIQUES APPLICABLE TO MASS SPECTROMETRY OF GASEOUS TRACE CONTAMINANTS

By Peter Warneck

GCA CORPORATION
GCA TECHNOLOGY DIVISION
Bedford, Massachusetts

FINAL REPORT

Contract No. NAS12-641

June 1970

Prepared for

NATIONAL AERONAUTICS AND SPACE ADMINISTRATION
Electronics Research Center
Cambridge, Massachusetts

TABLE OF CONTENTS

TECHNIQUES APPLICABLE TO MASS SPECTROMETRY OF GASEOUS TRACE CONTAMINANTS

By Peter Warneck, GCA Corporation, GCA Technology Division, Bedford, Massachusetts

SUMMARY

This report describes the continuation of an investigation into the application of charge transfer as the ionizing process in the ion source of the mass spectrometer. The experimental setup was modified in order to eliminate the interaction of sample gas with the primary ion source. To this end a differentially pumped gap was incorporated between the charge transfer chamber and the discharge source which serves as the primary ion source. Thereby, the extent of interaction of the sample gas with the primary ion source was reduced by about two orders of magnitude. A further reduction can be achieved by a more efficient differential pumping arrangement.

Charge transfer mass spectra are given for the sample gases CO_2, N_2O, NH_3, NO_2, SO_2, CO, isobutyl alcohol and formic acid for singly charged krypton as the main primary ion. For the latter two a comparison of ion intensities is made with photoionization and electron impact mass spectra. The feasibility of utilizing negative preliminary ions for charge transfer was demonstrated for the process O^-, $O_2^- + NO_2 \rightarrow NO_2^- + O$, O_2. The feasibility of discriminating carbon monoxide in the presence of nitrogen by means of the mass number 28 signal was explored for krypton primary ions. A residual nitrogen ionization limits the detectable amount of CO in nitrogen to five parts per ten thousand. The origin of the residual nitrogen ionization was investigated. It is due in part to a residual interaction of sample gas with the discharge source boundary, and in part to a primary ion with sufficient internal energy, probably excited metastable Kr^+ ions.

The first source of nitrogen ionization can be reduced by an improved differential pumping arrangement. The second source was found to vary with discharge conditions. Low fields and high pressures minimize this latter source of N_2^+. If krypton ions are to be retained as the primary ions for the purpose of CO - N_2 discrimination, a more detailed investigation of primary ion sources will be required to determine techniques by which the contribution of excited ions can be eliminated.

I. INTRODUCTION

This report describes results obtained in the second phase of Contract NAS12-641, which is concerned with the detection of gaseous trace contaminants. The total study involved three areas which were pursued independently and are specified as follows: (1) the investigation of a cryogenic target holder for the GCA solids analysis mass spectrometer for the purpose of gas solidification and analysis, (2) a study of the feasibility of utilizing charge transfer as the source of sample ionization in a gas analytical mass spectrometer, and (3) an investigation of resonance scattering of xenon as a means for pressure gauge calibration in the ultra-high vacuum region. Of

these, items 1 and 3 were brought to a reasonable degree of completion during the first phase of the present program. For a detailed description and discussion of the results reference is made to a previous technical report (Ref. 1). Item 2, however, required additional effort, so that the second phase of the program was concerned predominantly with that aspect. Accordingly, the present report will describe and discuss the progress made in continuing the investigation of charge transfer mass spectrometry.

In the following Section (II) the concept of charge transfer mass spectrometry will be briefly reviewed, and the objectives of the present investigation stated. Subsequently, in Section III, experimental details are given for the modifications made in the apparatus. Section IV serves to present and discuss the experimental results. Finally, in Section V the present level of development is summarized.

II. BACKGROUND INFORMATION AND SCOPE OF INVESTIGATION

The principles underlying the concept of charge transfer mass spectrometry may be briefly described: An ion moving in a gas mixture interacts with neutral particles in two ways: (a) by charge transfer and (b) by chemical interactions. The first type of process can occur only if the ionization potential of the neutral particle is less than the energy liberated by the neutralization of the ion. If this is the case, and ion velocities are nearly thermal, charge transfer occurs with high probability. The second type of process, chemical interaction also requires energetically favorable conditions. In this category fall the transfer of an atom, a group of atoms, or a general rearrangement of the molecular components with or without charge transfer. Frequently, they are as rapid as simple charge transfer, unless the process is endothermic. Proton transfer and hydrogen abstraction may be cited as examples for fast processes.

While both types of ion-neutral interactions can be utilized to form ions characteristic of the (neutral) sample gas mixture, the present work has emphasized simple charge transfer as a promising and generally applicable technique for sample gas ionization. The selection of primary ions with sufficiently low recombination energies makes it possible in principle, to ionize a sample without excessive fragmentation of the secondary (sample) ion. The resulting ion spectrum thus features predominantly parent ions, and the occurrence of fragment ions is greatly reduced. In this manner, the mass spectra of complex gas mixtures are simplified and their analysis is facilitated. Herein lies a principal advantage of the charge transfer ion source and its application to analytical mass spectrometry.

The present program extends an exploration into the feasibility of a charge transfer ion source. Basically, the source design incorporates two components: a source of primary ions and a chamber which the primary ions traverse and in which the charge transfer reactions take place. Both primary ions and secondary ions leaving the charge transfer region are subsequently processed with a mass analyzer. In the present study singly charged krypton ions were employed as the principal primary ions. For convenience, the primary ions are produced in a discharge source. Previously, the discharge region was mounted directly adjacent to the charge transfer chamber containing the sample gas. The results of a series of experiments performed with this source arrangement had indicated that the functional behavior of the secondary ions and the sensitivity of the technique were generally in agreement with expectation, but that ionization processes other than charge transfer occurred also. One important source of ionization appeared to be the interaction of the sample gas with the boundary of the discharge penetrating into the charge transfer chamber due to the gas flow. To eliminate this undesirable side effect, a more complete separation of the discharge region from the charge transfer region was desirable. Accordingly, the source design was modified to include a differentially pumped gap between the discharge region and the charge transfer space. Test results obtained with this modified source arrangement are reported further

below. A second problem that may be briefly mentioned is due to impurities, particularly water given off by the walls of the system and contained in the carrier gas. This problem could not be eliminated in the course of the present work because it required provisions for baking the entire source. The source modifications necessary to allow baking were beyond the scope of the present program and were not attempted.

III. EXPERIMENTAL DETAILS

The design criteria for the charge transfer ion source were described previously (Ref. 1). A feasibility model source had been built accordingly. The incorporation of a differentially pumped gap between the discharge and the sample ionization chamber resulted in the modified layout shown in Figure 1. A major experimental requirement is that the ions leaving the discharge source do not suffer collisions with neutral particles while crossing the gap region. The maximum tolerable pressure was found to be about 1 millitorr. Since both the discharge and the charge transfer chamber emit a gas flux through the orifices required for the withdrawal and injection of ions, a rather efficient pumping unit is needed. The 4-inch diffusion pump employed for the evacuation of the ion acceleration region behind the exit orifice of the charge transfer chamber supplied a sufficient pumping capacity, but the gap region could not be connected directly to the main ion source housing evacuated by the pump because of space limitations. Instead, a less efficient external pump connection had to be tolerated. This approach allowed the re-use of the existing components of the ion source. The differentially pumped gap is contained in a 1-inch thick spacer flange provided with a 1-inch diameter pump lead. The discharge ion source is mounted onto an aluminum cover plate which in turn is insulated from the body of the charge transfer ion source by a nylon spacer flange. A variable potential of 0 - 150 volts between the discharge source exit and the charge transfer chamber plates was provided, but was not found critical in obtaining adequate primary ion intensities. Similarly, it was initially attempted to focus the primary ions onto the entrance aperture of the chamber by an additional ring electrode in the differentially pumped gap. The gain was found to be less than a factor of two so that the electrode was later omitted. The exit orifice of the discharge source was made 0.06 cm in diameter to match it with the entrance aperture of the charge transfer chamber. The axial position of the discharge end plate was variable. However, no attempts were made to optimize it.

The other components of the apparatus were left unchanged. Briefly, primary and secondary ions emerge from the charge transfer region through a 0.14 cm diameter orifice due to the action of a weakly converging field inside the chamber, and are accelerated and focused onto the entrance aperture of a 180 degree magnetic analyzer by an assembly of stainless steel plates forming an immersion lens system. After passage of the mass analyzer the ions are either collected in a faraday cage and registered with an electrometer, or processed with a secondary electron multiplier detector prior to registration.

The gas inlet serving the discharge tube was the same as that used previously (Ref. 1). Before entering the discharge the gas passed a liquid nitrogen cold trap to reduce the contamination by water vapor. The sample gas inlet to the charge transfer chamber was supplemented with a second inlet and control valve for the introduction of a buffer gas. In all experiments the buffer gas was the same as that used in the discharge.

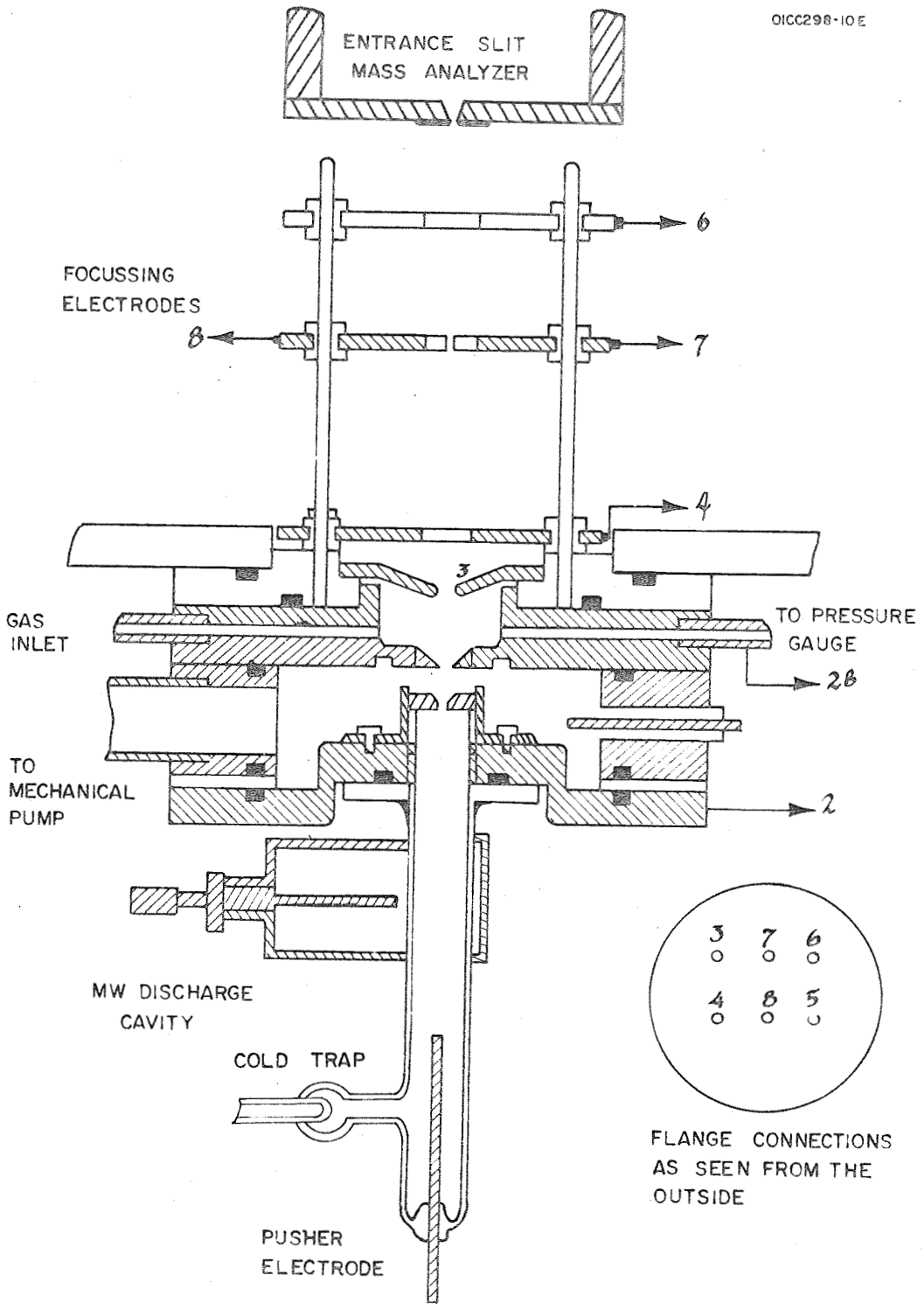

Figure 1. Charge transfer ion source.

IV. RESULTS

A. Primary Ion Intensities and Sensitivities

Previously, the primary discharge ion source had been operated either as a dc cold cathode discharge, or by way of microwave excitation. In the latter mode, an air-cooled Evenson cavity was used in conjunction with a 100 Watt Microtherm unit to supply the electric field. The microwave excitation provided higher ion intensities, but led also to a considerable penetration of the discharge plasma into the charge transfer region thereby causing a direct ionization of the sample gas (Ref. 1). This effect was completely eliminated by the differentially pumped gap. Since higher ion intensities are derived from the microwave discharge, all the experiments reported below were performed with microwave excitation.

Due to the spread of the ion beam emerging from the primary (discharge) ion source only a portion of the total emitted ion current enters into the charge transfer chamber. Accordingly, a smaller primary ion intensity is anticipated in comparison with previously established values. However, these losses were not serious. Primary ion currents transmitted through the charge transfer chamber (at low pressures in this region) and measured at the entrance of the mass analyzer were, typically, 4×10^{-10} amps for krypton ions. With about 0.1 torr of krypton in the charge transfer chamber, the transmitted primary ion intensity decreased to about 1.5×10^{-10} amps. The corresponding loss of ion intensity inside the charge transfer chamber due to spreading of the entering ion beam is much less than that observed previously when the discharge ion source was connected directly to the charge transfer chamber.

From this observation and on the basis of comparable sample ionization efficiencies one expects equivalent sensitives. Indeed, the measured sample gas sensitivities are similar to those established with the previous source configuration as is shown in Table 1, for approximately equal pressure and field conditions in the charge transfer region. It has already been noted previously, that the sensitivies achieved with the present device are about three orders of magnitude lower than those obtained with electron impact ionization. However, the usable sample pressures in the ion source are about three orders of magnitude higher, so that the lower sensitivity is compensated and ion currents comparable to electron impact ionization are achieved.

B. Charge Transfer Mass Spectra

To illustrate the kind of mass spectra observed with the charge transfer ion source, we present in Figures 2 through 5 the spectra observed when small amounts of SO_2, N_2O, CO or ammonia are admixed to krypton in the charge transfer chamber. The primary ions were derived from a krypton discharge and consisted mainly of singly charged krypton which appears at

TABLE 1

SENSITIVITIES OF CHARGE TRANSFER ION SOURCE
FOR VARIOUS SAMPLE GASES USING Kr^+ AS PRIMARY ION

SAMPLE GAS	MASS OF PARENT PEAK	SENSITIVITY (10^{-8} amps/torr) PRESENT	PREVIOUS
Carbon Dioxide	44	2.0	1.2
Nitrous Oxide	44	2.0	1.8
Sulfur Dioxide	64	5.0	8.3
Oxygen	32	0.3	-
Ammonia	17	6.0	6.1
Carbon Monoxide	28	0.35	-

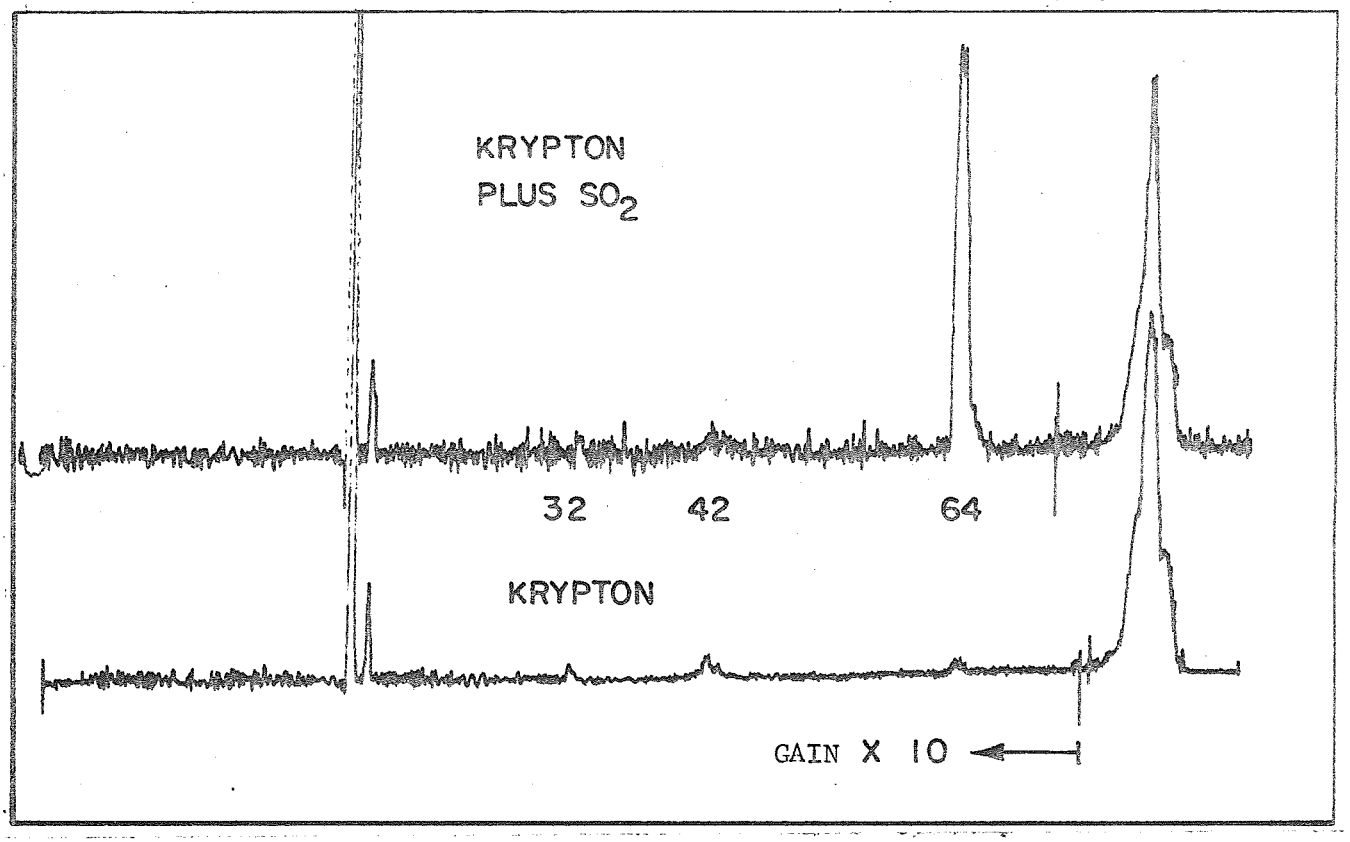

Figure 2: Charge transfer mass spectrum of sulfur dioxide

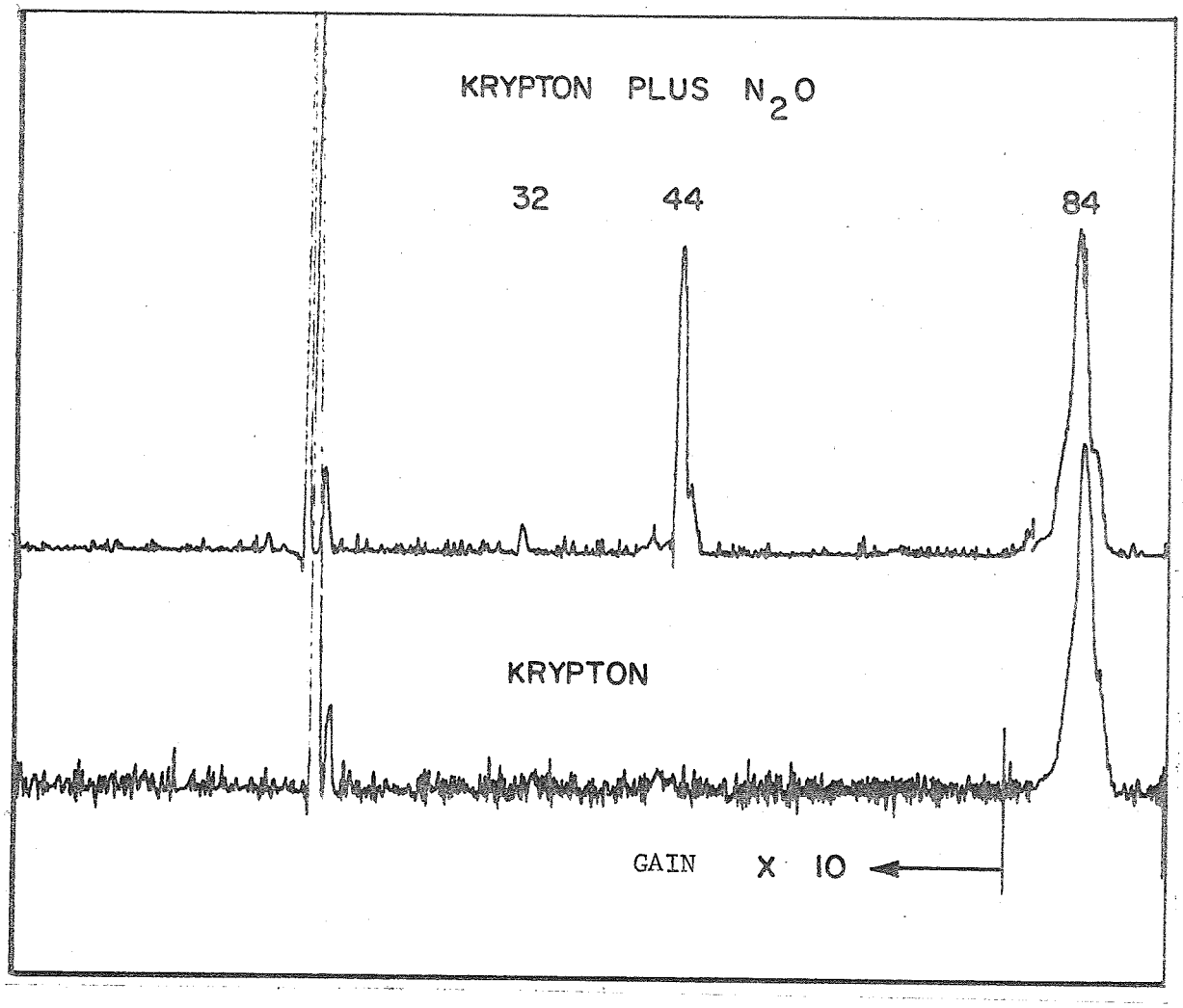

Figure 3: Charge transfer mass spectrum of nitrous oxide

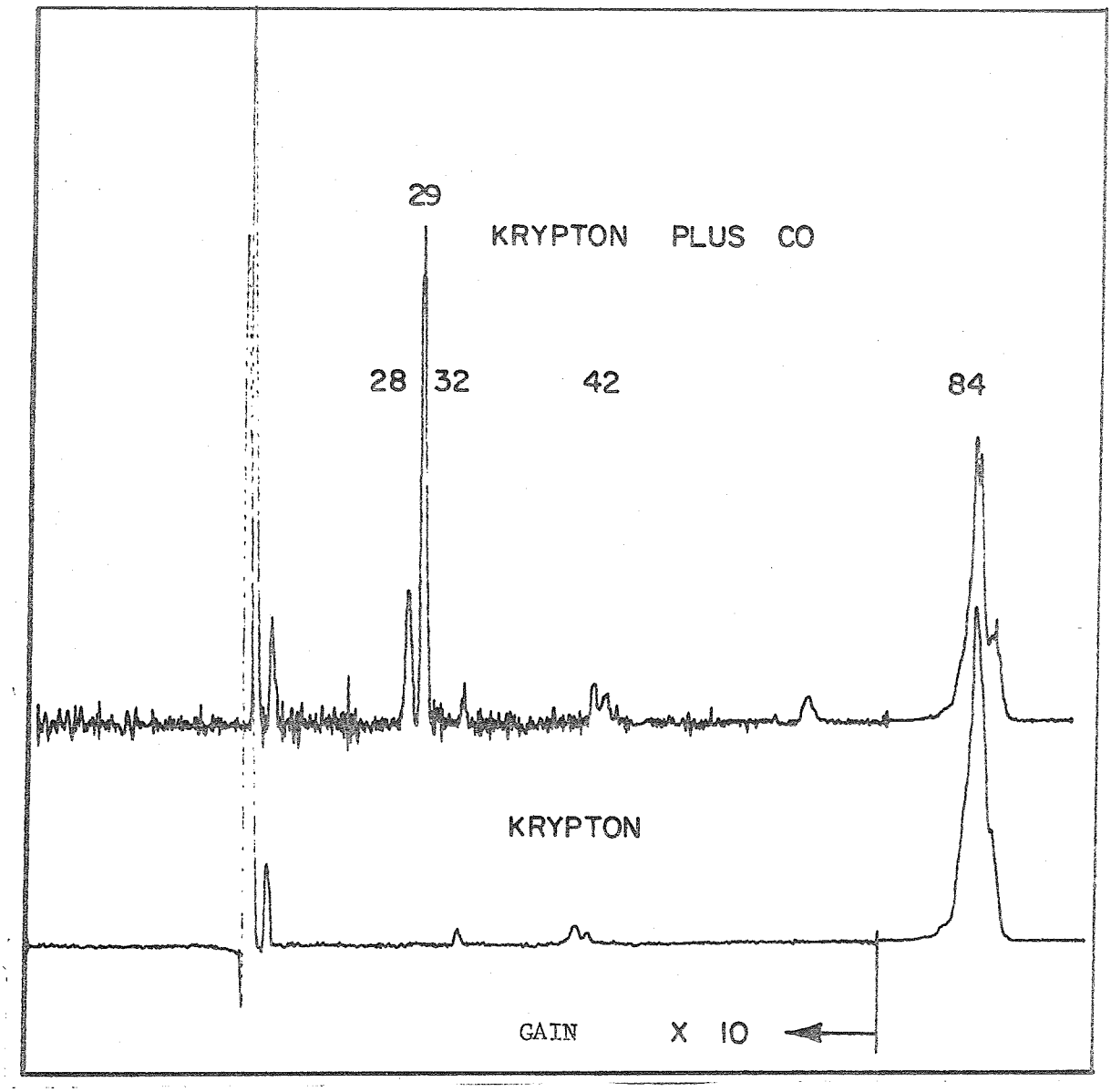

Figure 4: Charge transfer mass spectrum of carbon monoxide

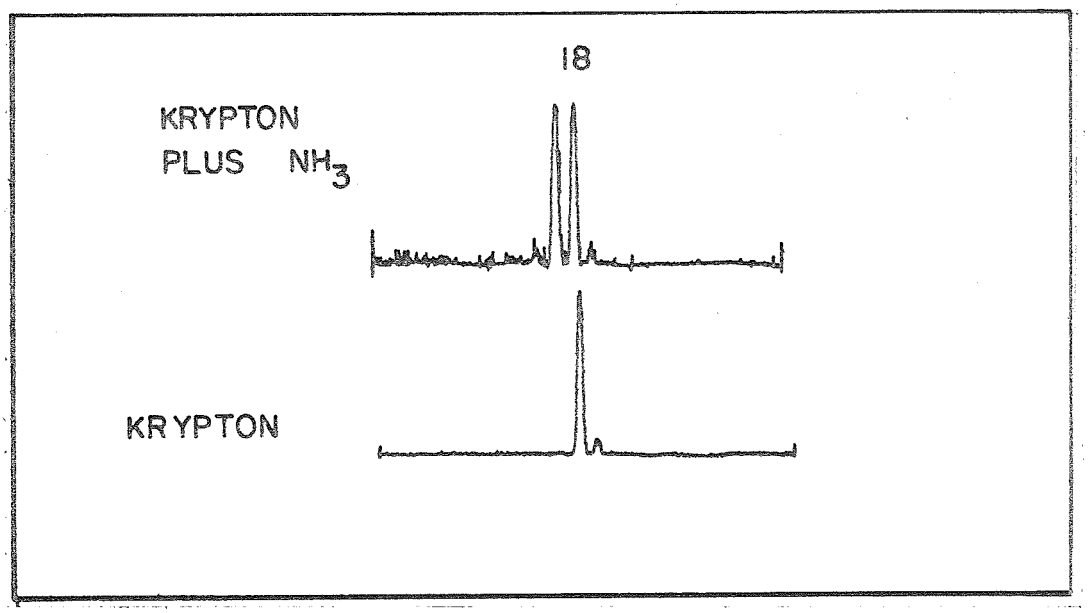

Figure 5: Charge transfer mass spectrum of ammonia

mass number 84 with an isotopic distribution ranging from 80 to 86 atomic mass units. However, some doubly ionized krypton and krypton hydride ions were also present as indicated by the signals at mass number 42 and 85. In addition to the primary ions, the background spectrum contains O_2^+ at m/e = 32 and H_2O^+ and H_3O^+ at mass numbers 18 and 19 respectively. These ions originate from impurities. New peaks appear upon the introduction of sample gases.

Sulfur dioxide and nitrous oxide give rise to the peaks at 64 and 44 atomic mass units, respectively. These are the parent peaks. No fragment ions are observed, but the parent peaks show tails toward higher mass numbers indicating the presence of protonated SO_2 and N_2O.

The introduction of ammonia leads to the expected M17 parent ions. In addition, an ion occurs also at mass number 16, probably representing the NH_2^+ fragment. The appearance potential for NH_2^+ from ammonia has been given as 15.8 eV. Hence, this ion is not expected to be produced by simple charge transfer from singly charged krypton ions. The introduction of carbon monoxide gives rise to two peaks at mass numbers 28 and 29. The first of these is the CO parent peak, whereas the latter is COH^+, the protonated species. It is interesting that in contrast to SO_2 and N_2O the mass 29 signal is much greater than the parent ion signal. Apparently, direct charge transfer is not as effective as proton transfer by krypton hydride.

$$(1) \qquad Kr^+ + CO \rightarrow CO^+ + Kr$$

$$(2) \qquad KrH^+ + CO \rightarrow COH^+ + Kr$$

It should be noted that direct charge transfer is slightly endothermic (by 0.02 eV) for krypton ions in the ground state, so that it may be less efficient than for exothermic processes. The sensitivity data in Table 1 show that CO behaves similar to O_2 for which charge transfer is exothermic. However, the sensitivities for both O_2 and CO are lower than that for other molecules, notably CO_2 which has a similar ionization potential. Hence, it seems that the low sensitivity of CO is due more to the lower efficiency of charge transfer than to the small endothermicity of the process.

The process of proton transfer resulting in COH^+ is quite efficient as evidenced by the strong signal on mass number 29. A portion of the signal apparently is due to the process

$$(3) \qquad CO^+ + H_2O \rightarrow COH^+ + OH$$

because the ratio of the peaks at mass numbers 28 and 29 varied with the focusing conditions and with the electric field applied to the charge transfer chamber. The former controls the location from which ions are sampled; the latter varies the residence time of primary and secondary ions in the

chamber. Table 2 shows that the CO^+ signal increases with increasing drift voltage whereas the COH^+ and the O_2^+ signals decrease. Since the CO^+ signal decreases only by a factor of five, while the COH^+ signal (and the O_2^+ signal) increases by more than a factor of twenty, it is evident that reaction (3) only supplements COH^+ formation by proton transfer.

In addition to the spectra observed for the inorganic compounds discussed above, further spectra were obtained for iso-butyl alcohol and for formic acid as examples for organic compounds with low ionization potential. Representative spectra are shown in Figures 6 through 9. Two types of primary ions were employed: (a) krypton ions from a krypton discharge, and (b) ions from a discharge through oxygen. In the second case, the major primary ions are O_2^+, with an ionization potential of 12.02 eV and O^+, having an ionization potential of 13.5 eV. Charge transfer to iso-butyl alcohol from both krypton and oxygen primary ions, produces extensive mass spectra which are characterized by considerable fragmentation (Figures 6 and 7). The ionization potential of iso-butyl alcohol is 9.93 eV, so that fragmentation by ions of greater recombination energy is not unexpected. In fact, both photoionization (Ref. 2) and electron impact ionization (Ref. 3) also result in considerable fragment ion formation. A comparison of such data is given in Table 3. It is interesting to observe that charge transfer using oxygen as primary ions gives a spectrum quite similar to photoionization with radiation of 15.4 eV energy, whereas charge transfer from krypton ions results in a spectrum which compares better with the spectrum produced by electron impact. Noteworthy in the latter case is the low intensity of the parent ion peak.

A similar situation occurs with formic acid. Spectra obtained with krypton and oxygen primary ions are shown in Figures 8 and 9. The observed ion intensities are compared in Table 4 with those produced by photoionization (Ref. 2) and electron impact (Ref. 4). Again, charge transfer from oxygen ions resembles ionization by 15.4 eV photons, whereas charge transfer from krypton ions producesa spectrum more like that observed with electron impact. The spectra obtained by charge transfer using oxygen primary ions are approximately in accord with expectation, but charge transfer from krypton appears to produce more highly fragmented ion spectra than anticipated. No explanation can be given for this behavior at the present time.

C. Negative Ions

While the majority of the experiments in this program were concerned with charge transfer involving positive ions, it is obvious that a similar phenomenon should occur also with negative ions. Negative ion mass spectra are often simple and less extensive than the positive ion mass spectra of the same compounds, so that it was of interest to explore charge transfer using negative ions with the present experimental set-up. This involved

TABLE 2

VARIATION OF M28 AND M29 SIGNALS
WITH DRIFT POTENTIAL FOR CO SAMPLE GAS

Drift Potential, v	1/v	Peak Height M28	Peak Height M29	Ratio 28/29	Peak Height M32
50	0.020	71	48	1.5	14
35	0.028	60	118	0.6	29
23	0.043	30	510	0.06	150
16	0.062	15.6	1050	0.015	360

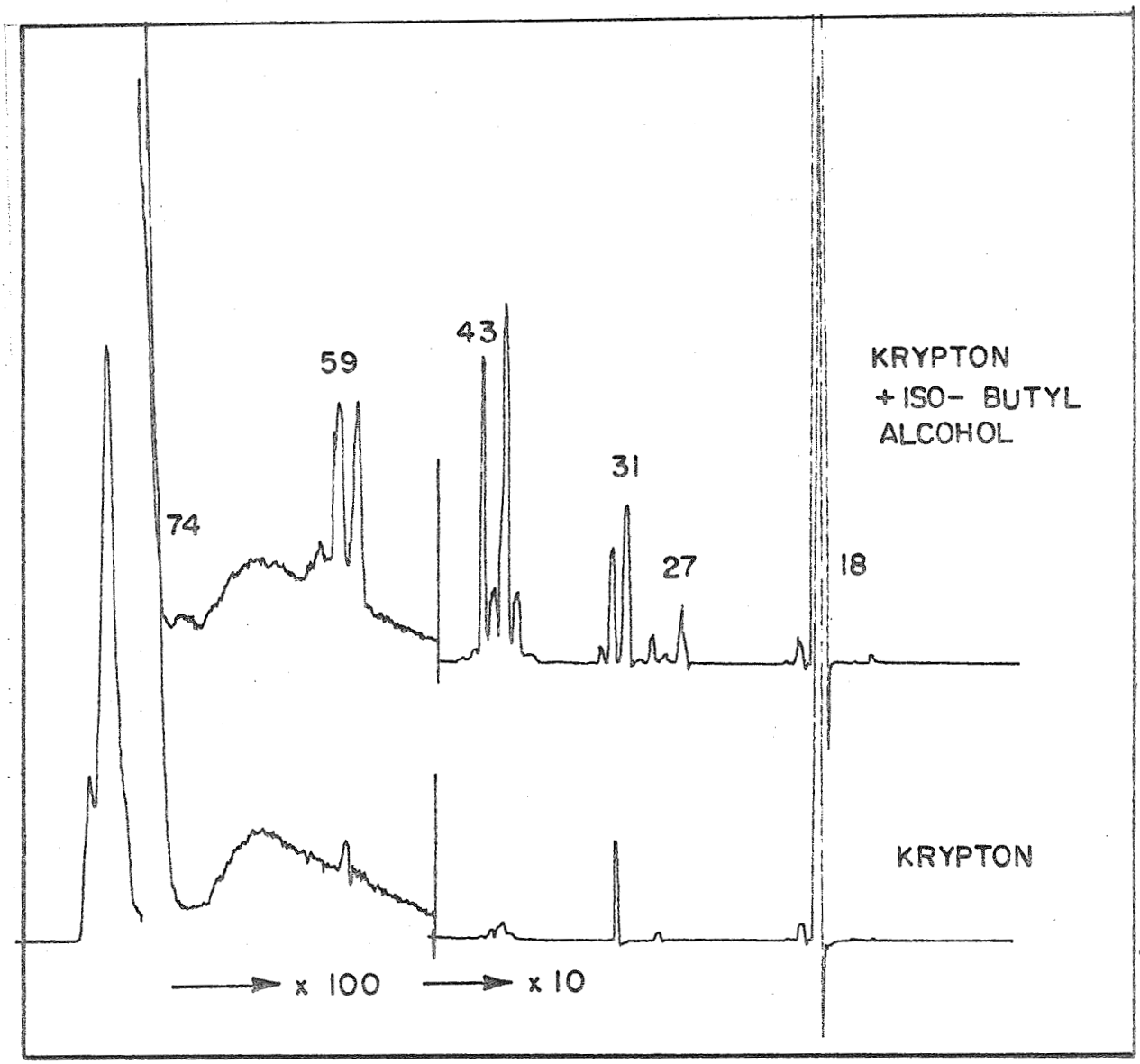

Figure 6: Charge transfer mass spectrum of iso-butyl alcohol, krypton primary ions.

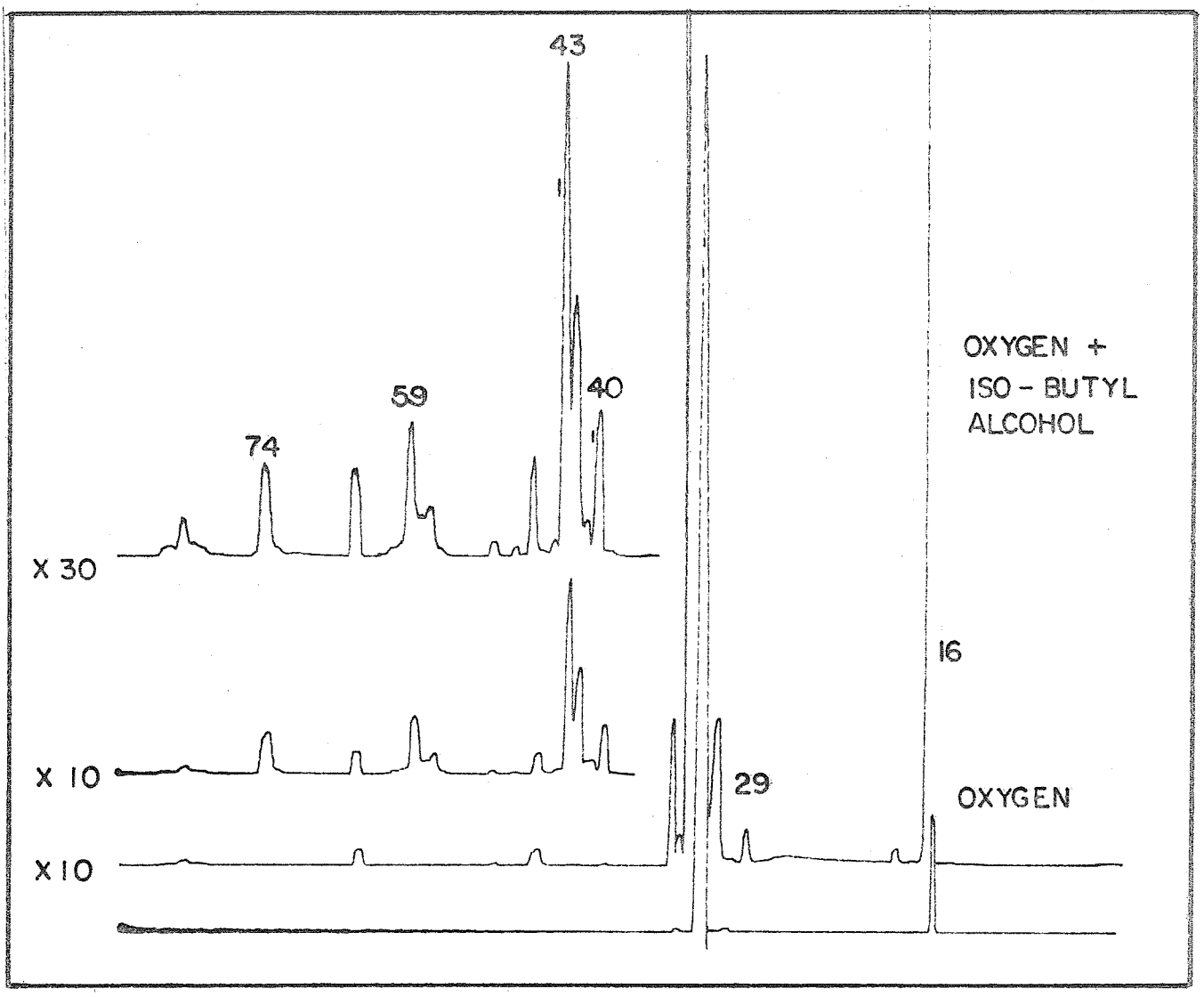

Figure 7: Charge transfer mass spectrum of iso-butyl alcohol. Oxygen primary ions.

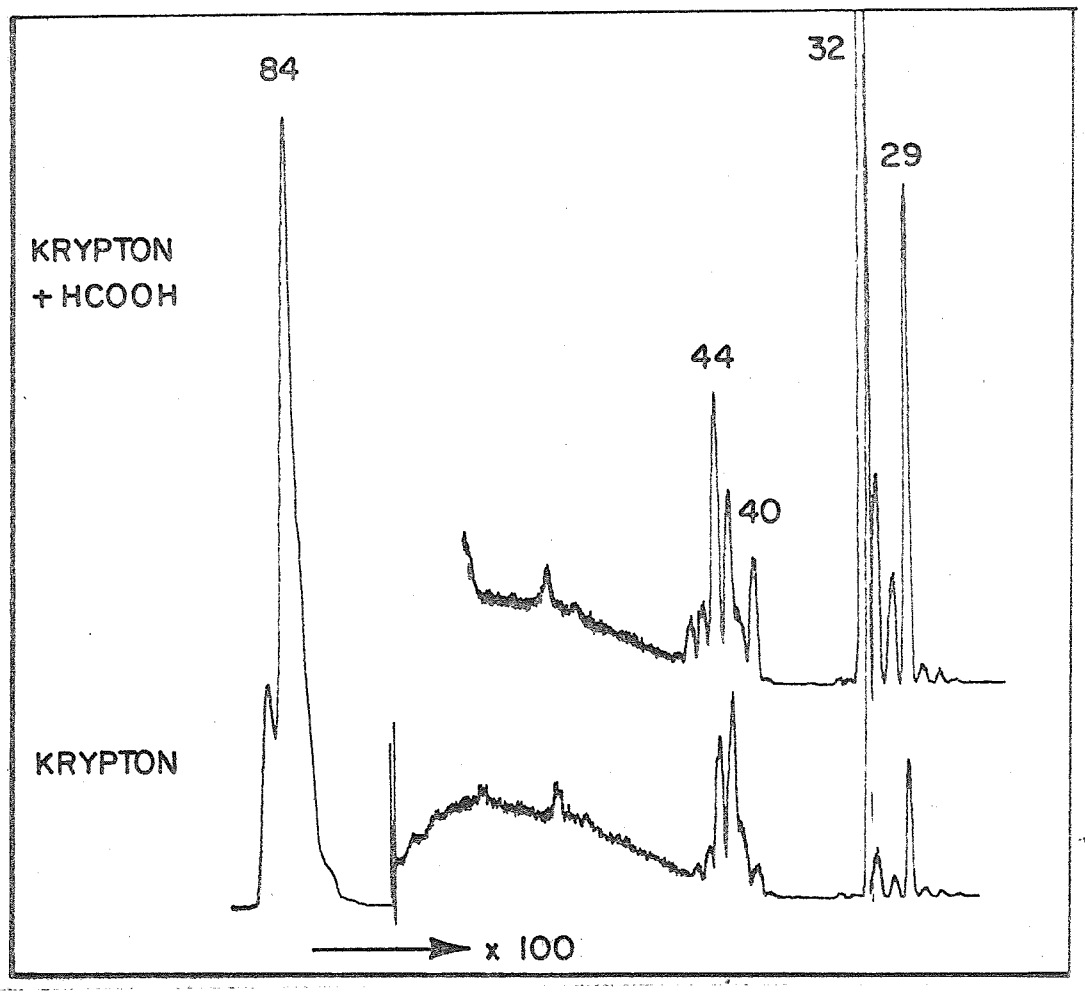

Figure 8: Charge transfer mass spectrum OH Formic Acid. Krypton Primary Ions.

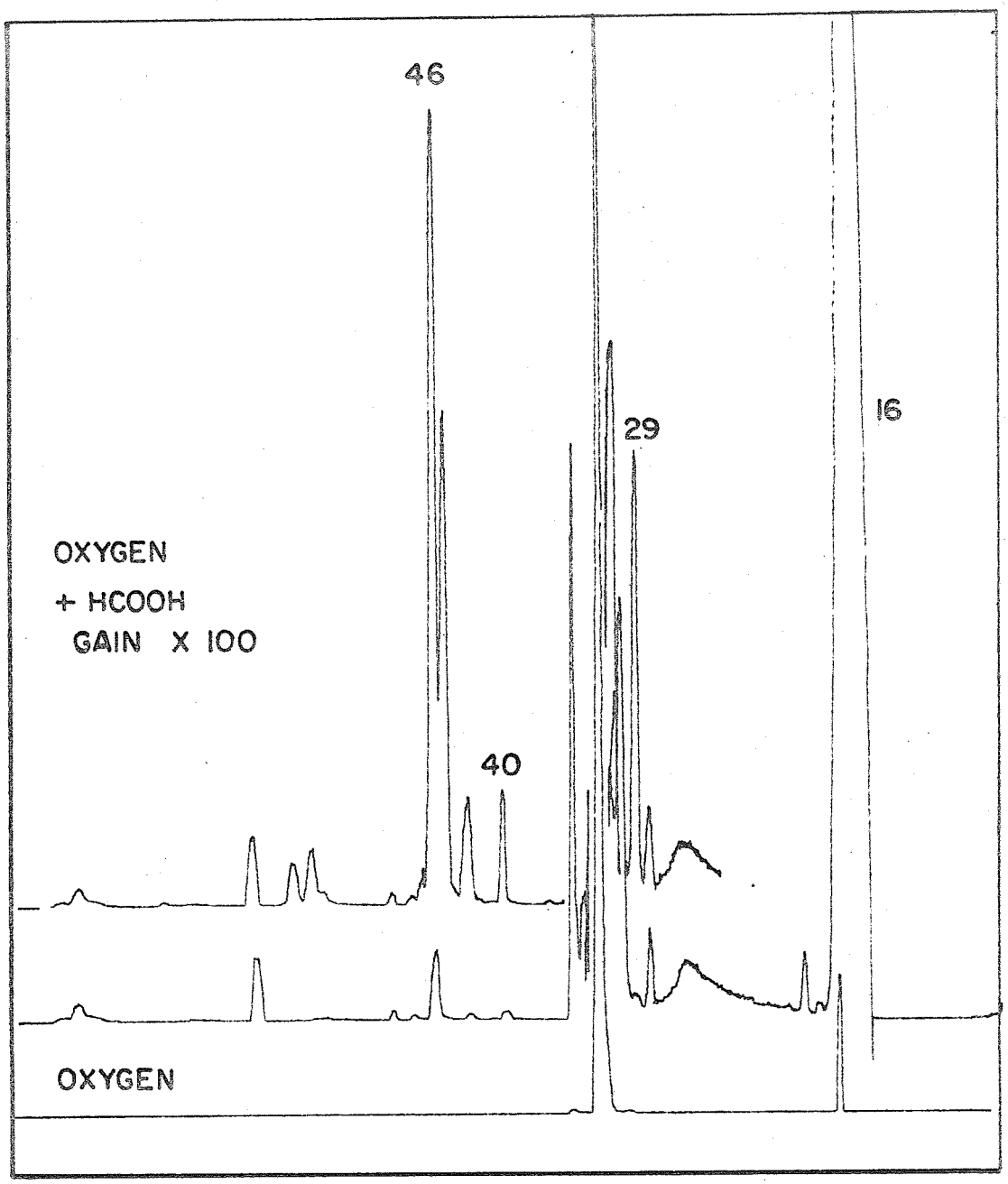

Figure 9: Charge transfer mass spectrum of formic acid. Oxygen primary ions.

TABLE 3

RELATIVE ION YIELDS FOR ISO-BUTANOL
BY VARIOUS MODES OF IONIZATION

MASS NO	PHOTOIONIZATION 13.0 ev	PHOTOIONIZATION 15.4 ev	ELECTRON IMPACT IONIZATION 70 ev	CHARGE TRANSFER Kr^+	CHARGE TRANSFER O_2^+/O^+
74	30	19	9	0.4	18
59	5	4	5	6	27
57	9	8	4	6	10
43	100	100	100	100	100
42	79	63	57	19	47
41	8	47	56	100	8
33	84	60	53	6	-
31	15	34	63	43	-
27	1	10	43	13	-

TABLE 4

RELATIVE ION YIELDS FOR FORMIC ACID
BY VARIOUS MODES OF IONIZATION

MASS NO	PHOTOIONIZATION 15.4 ev	ELECTRON IMPACT 70 ev	CHARGE TRANSFER Kr^+	CHARGE TRANSFER O_2^+/O^+
46	100	61	10	100
45	62	48	8	61
44	-	10	30	-
30	6	-	23	10
29	22	100	100	55
28	-	17	2	-

reversing all potentials as well as the magnetic field. Oxygen was used in the gas discharge ion source. The primary ion spectrum under these conditions consisted mainly of O^-, with O_2^- being present at a lower intensity. The total primary ion intensity obtained in this manner was about a hundred times lower than for positive ions. The reasons for the lower efficiency of the ion source for negative ions lies in the problems associated with the extraction of negative ions through the plasma sheath surrounding the discharge region. Usually, an additional electrode is positioned in front of the anode disc to increase the efficiency of negative ion extraction (Refs. 5, 6). The present ion source was not provided with this feature, so that the comparatively low primary ion current had to be tolerated.

To demonstrate the effect of charge transfer, nitrogen dioxide was employed as the sample gas. Figure 10 shows typical results obtained in the presence and absence of NO_2 in the charge transfer chamber. The signal at mass number 46 indicates that charge transfer occurs with a reasonable efficiency, as expected from the known rate coefficient (Ref. 7) for the reaction

$$(4) \qquad O^- + NO_2 \rightarrow NO_2^- + O$$

The NO_2^- ion is the only secondary ion produced. The positive ion spectrum, by comparison, produces not only NO_2^+, but also NO^+ at m/e = 30 with oxygen primary ions. A representative positive ion mass spectrum is shown in Figure 11. The comparison shows that even for this simple case of NO_2, the negative ion charge transfer possesses advantages. However, its application requires a more efficient negative ion source.

D. Sources of Ionization Other than Charge Transfer

From the results discussed above, it appears that the ion source in its present configuration which includes the differentially pumped gap between the primary ion source and the charge transfer region is superior to the previous source arrangement without the gap, as fragment ion formation due to interaction of the sample gas with the discharge boundary has been essentially eliminated. While this is true for the gases N_2O, SO_2, CO and NH_3 which were also studied previously, specific reference is made to SO_2 for which mass spectra were published so that a direct visual comparison can be made. The qualitative appearance of mass spectra, however, does not provide a quantitative measure of the improvement attained. To determine the degree to which the formation of undesirable ions is suppressed, a variety of further experiments were carried out employing nitrogen as the sample gas and primary ions derived from a krypton discharge. The choice of nitrogen as sample gas was made for two reasons: (a) it was used as test gas in previous experiments without the differentially pumped gap. Hence, the new data would provide a quantitative assessment of the

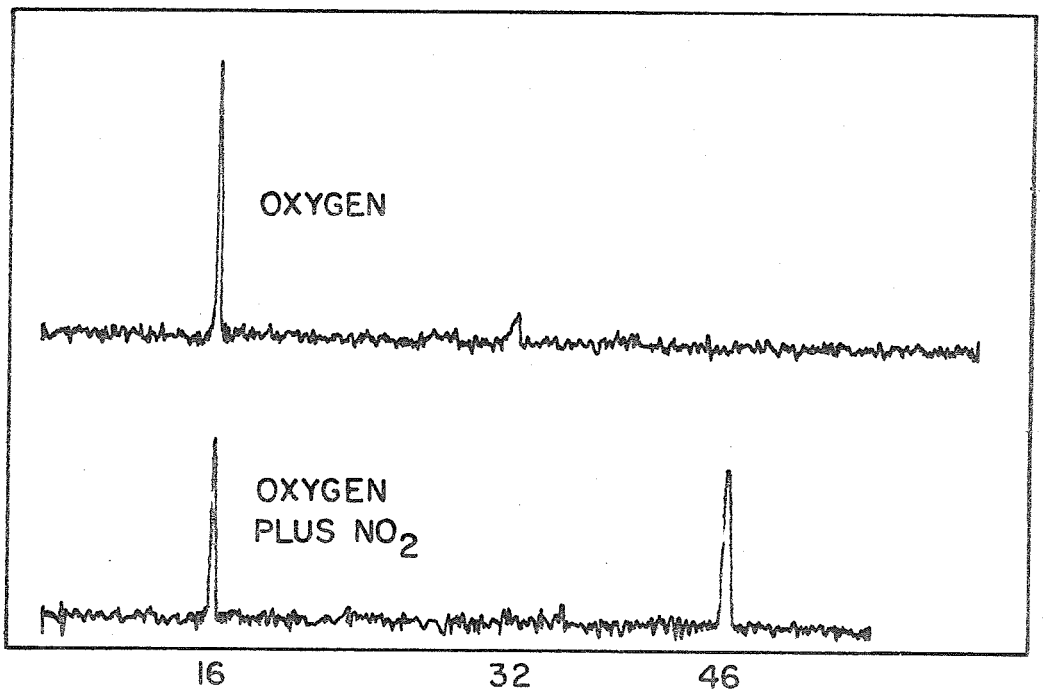

Figure 10: Charge transfer mass spectrum of nitrogen dioxide. Negative oxygen primary ions

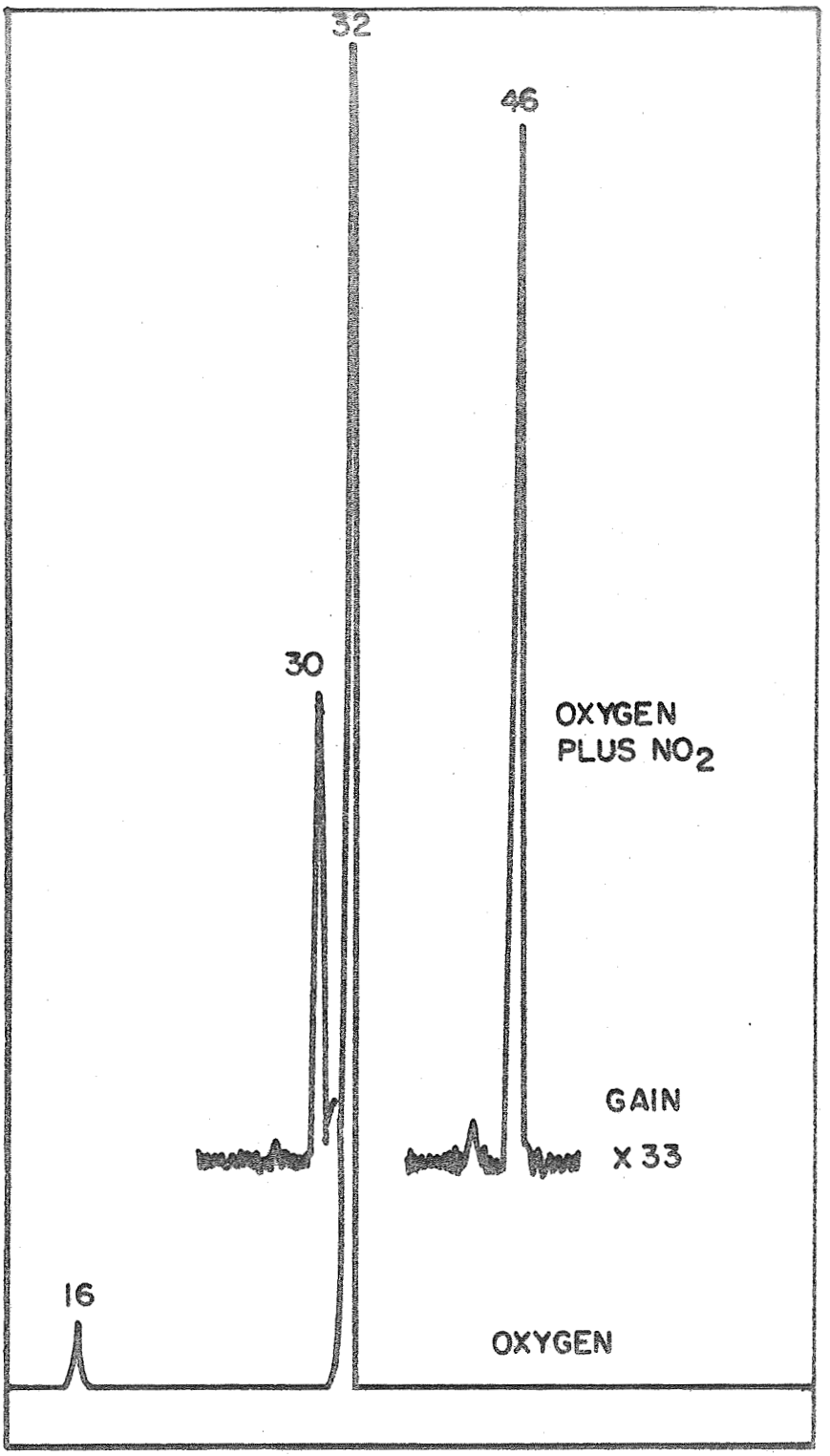

Figure 11: Charge Transfer Mass Spectrum of Nitrogen Dioxide, Positive oxygen primary ions.

source improvement; and (b) the N_2^+ signal coincides with that of CO^+ so that the possibility of detecting CO in air by charge transfer mass spectrometry may be evaluated. The ionization potential of nitrogen is such that singly charged ground state ions of krypton of low kinetic energy cannot ionize nitrogen due to an energy deficiency of about 1.5 eV. Nevertheless, both N_2^+ and N^+ had been observed previously. The sources of nitrogen ionization had been discussed and it was concluded that it occurred by interaction with the boundary of the discharge. Another potential source are doubly charged krypton ions which are generated in the primary source discharge as a minor ionic component.

The incorporation of the differentially pumped gap into the ion source arrangement was found to reduce the direct ionization of nitrogen considerably. Figure 12 shows a spectrum produced when 3×10^{-3} torr of nitrogen is added to 0.155 torr of krypton in the charge transfer region. There is a sizable signal on mass number 29, demonstrating the formation of N_2H^+, but no signals are evident on mass numbers 28 and 14. Comparison with the previous data indicates that the amount of N_2^+ formation has been reduced at least twenty-fold, whereas the contribution of N_2H^+ formation remains similar. The latter presumably is due to proton transfer from krypton hydride ions present in the primary ion distribution.

The spectrum in Figure 12 was taken on the most sensitive scale of the available electrometer and is accompanied by an appreciable background noise. Further investigation of nitrogen ionization thus required an increase of ion detection sensitivity and/or noise reduction. The noise level apparent in Figure 12 is due to the electrometer entrance circuit and cannot be reduced. Hence, to increase the signal-to-noise ratio, the simple Faraday cage ion collector was replaced by an electron multiplier detector which was adjusted to a gain of 10^4. With this modification sufficient sensitivity reserve was made available to detect the mass number 28 signal and to establish that its size was reduced by a factor of about 35 compared with previous data obtained under similar experimental conditions. The improvement attained clearly indicates that the bulk of the interaction between gas discharge and sampling gas has been removed by the differentially pumped gap.

Next it was desirable to lower the rather strong ion intensities due to water contamination. For this purpose, a second liquid nitrogen trap was installed in the inlet line feeding the buffer gas (krypton) to the charge transfer chamber. This modification led to a considerable reduction not only of the signals on mass numbers 18 and 19, which are directly related to the water vapor concentration in the charge transfer chamber, but also to a reduction of the m/e = 29 signal indicating that N_2H^+ formation is partially connected with the water impurity problem. The m/e = 28 signal was not affected by this measure. Typical spectra obtained for these experimental conditions are shown in Figure 13. It is noteworthy that with the increased gain a considerable number of impurity peaks become apparent.

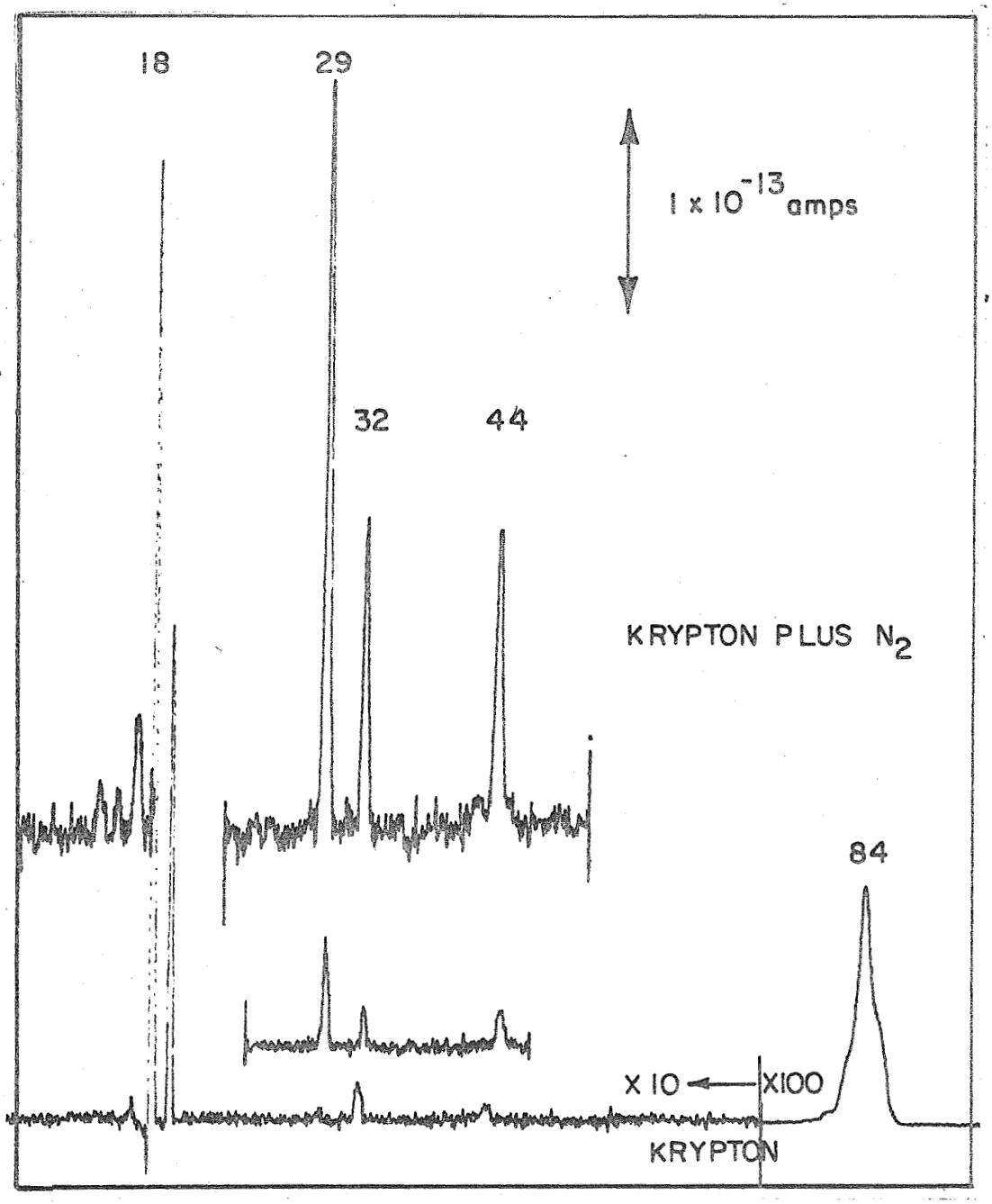

Figure 12: Spectrum produced by the addition of nitrogen to the charge transfer chamber.

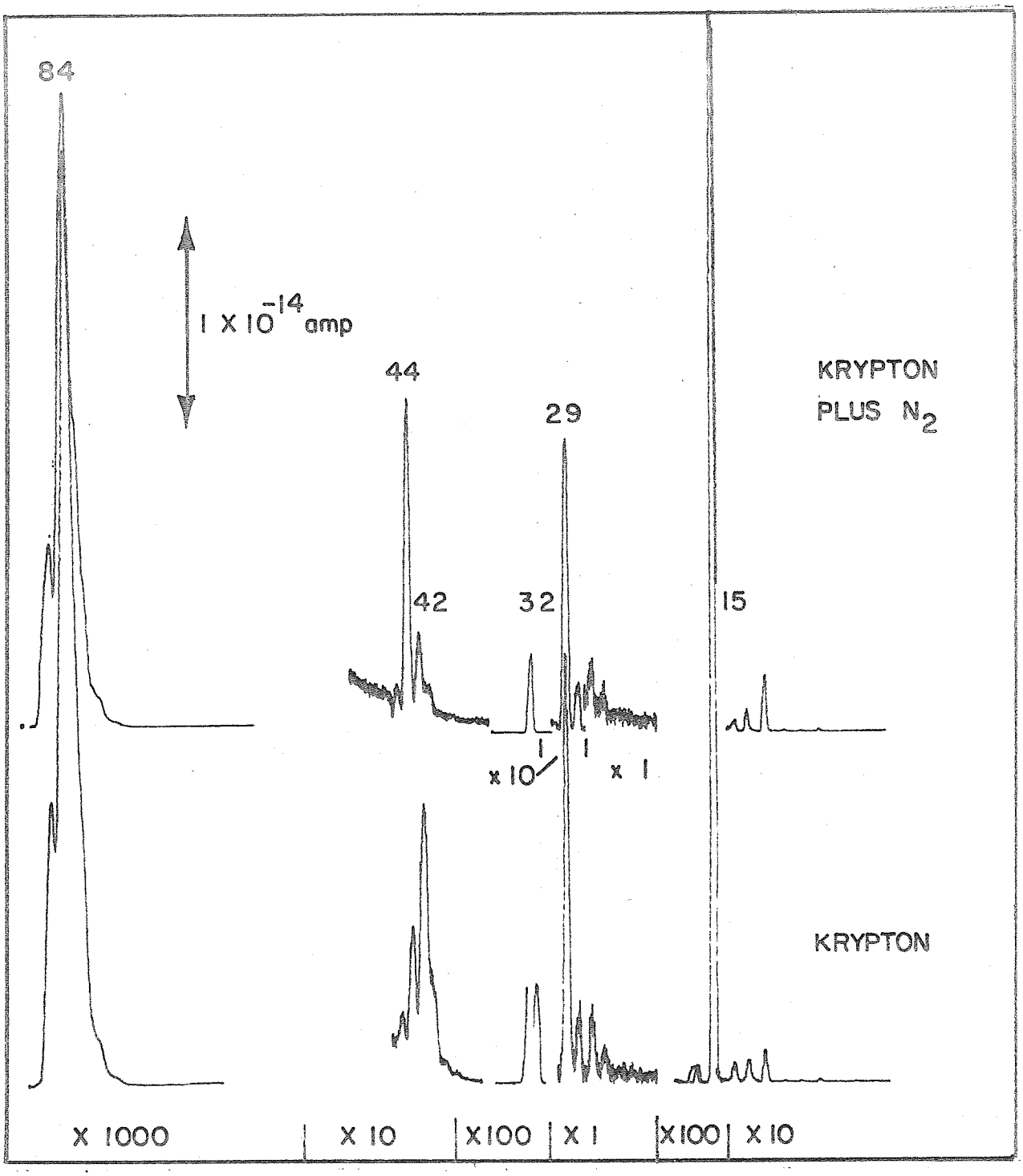

Figure 13: Mass spectrum produced by the addition of nitrogen to the Charge Transfer Chamber. Liquid N_2 traps in both krypton inlet lines.

These belong mainly to ions created by contamination in the discharge primary source, e.g., the peaks on mass numbers 27, 26, 25 and 15 are due to hydrocarbon ions, the peaks on mass numbers 16 and 17 are caused by water vapor. The increase in the signal at m/e = 15 when nitrogen is introduced to the charge transfer chamber indicates that a small amount of hydrocarbon is introduced through the nitrogen inlet. The increase in the signal at m/e = 44 can be attributed to the same source, i.e., a hydrocarbon rather than carbon dioxide, but the rise in the peaks at mass numbers 28 and 29 is much larger and must be due to nitrogen. If these signals were caused by a hydrocarbon, the peaks at mass number 27 and 26 should increase also by a proportionate amount whereas they remain constant. Accordingly, the signals observed on mass numbers 28 and 29 when nitrogen is admitted to the charge transfer chamber are attributed to the ions N_2^+ and N_2H^+, respectively.

To determine the origin of the residual N_2^+ formation a variety of further experiments were performed. Figure 14 shows that the intensity of ions appearing at mass numbers 32, 29 and 28 increase with the partial pressure of nitrogen. The increase is essentially linear although for both M28 and M29 some saturation occurs at N_2 pressures greater than 40 microns. This behavior is probably caused by tertiary reactions of both N_2^+ and N_2H^+ with water vapor, rather than a partial depletion of the primary ions responsible for their formation.

Figures 15 and 16 show the variation of ion intensities observed when the krypton pressure in the charge transfer chamber is varied in the absence or presence of a constant nitrogen pressure. In both cases, the M32 and M29 ion intensities show an essentially linear increase with pressure, whereas the M28 ion intensity stays approximately constant. The linear increase with buffer gas pressure is due to the increase in the residence time of the primary ions and is in accord with the functional relationship derived previously. This type of intensity dependence is now shown more clearly than by the previous source arrangement because in the present setup the primary source and the charge transfer chamber parameters can be varied independently.

Figure 15 thus shows that the M32 and M29 ions are true secondary ions formed by the processes

$$(5) \qquad Kr^+ + O_2 \rightarrow O_2^+ + Kr$$

$$(6) \qquad KrH^+ + N_2 \rightarrow N_2H^+ + Kr$$

whereas the M28 ion assigned to N_2^+ behaves abnormally as a secondary ion. The proportionality of the M28 ion intensity with the nitrogen partial pressure demonstrates it to be formed directly from nitrogen, but does not indicate the process responsible for it. If it is formed in the charge transfer region it must be produced by a sufficiently energetic ionic process, such as charge transfer involving either Kr^{++} or metastable excited Kr^+ ions. However, one must also consider the possibility that N_2^+

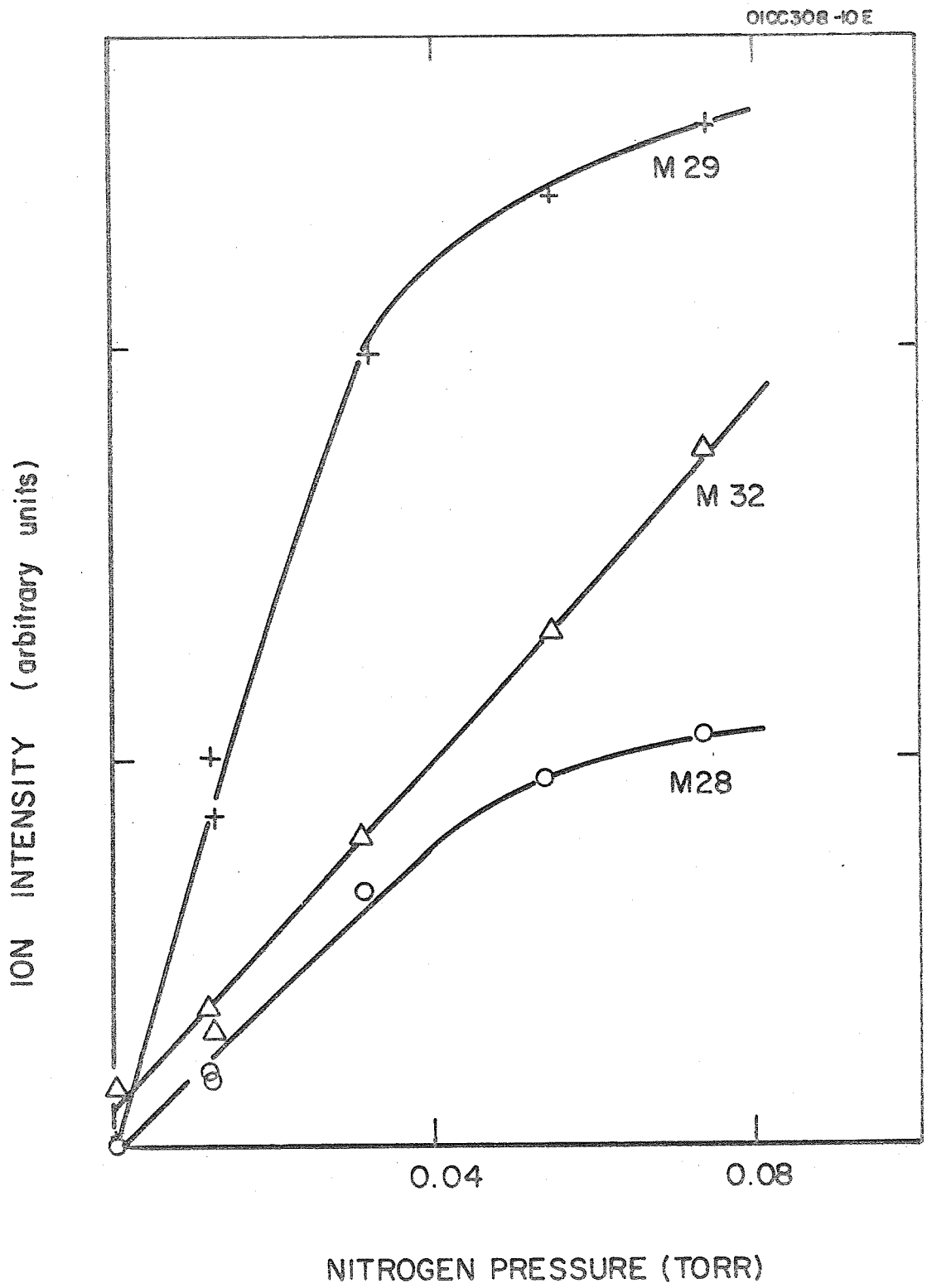

Figure 14. Dependence of ion signals on sample pressure

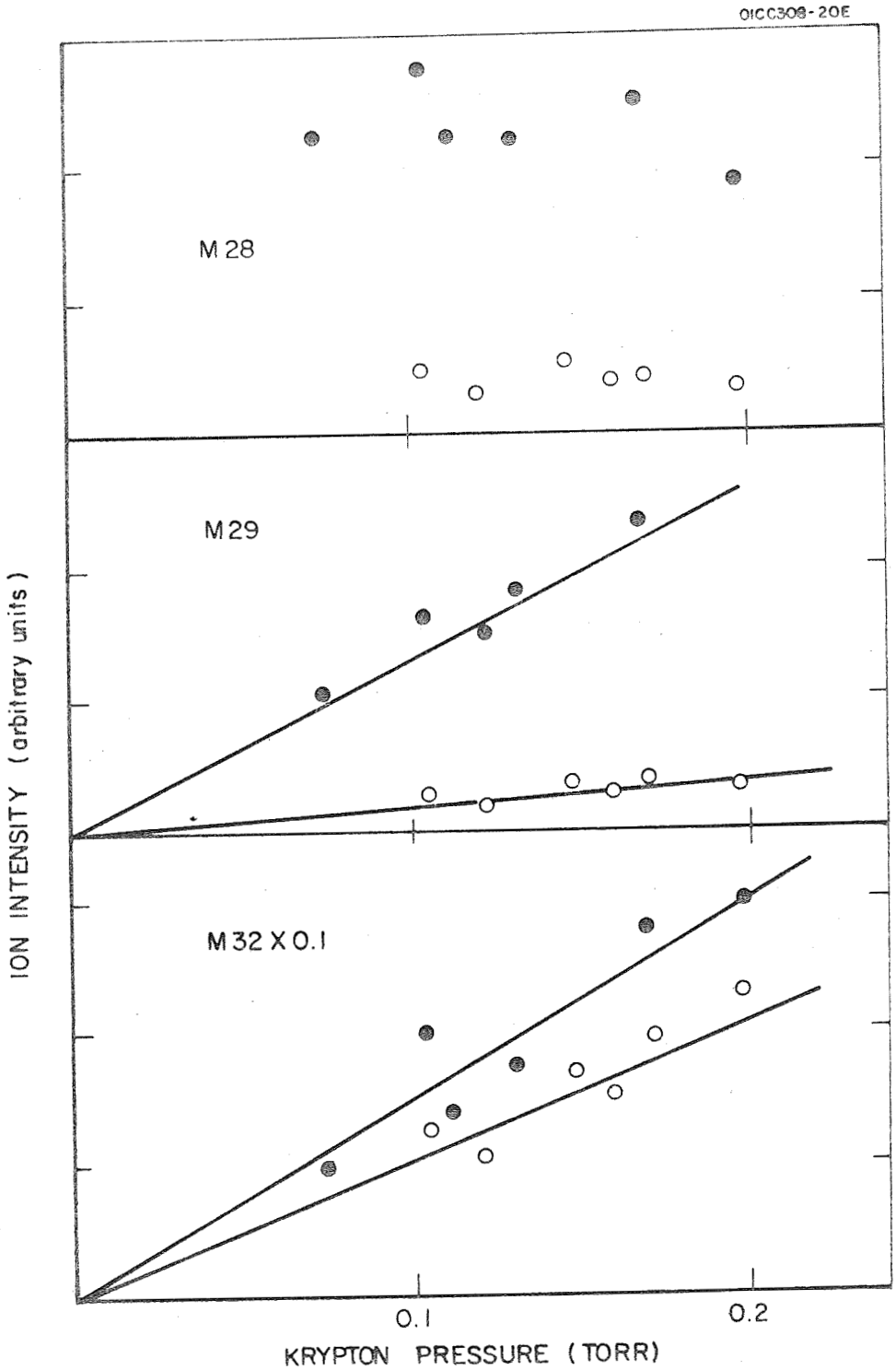

Figure 15. Variation of ion signals with the presence of krypton in the charge transfer chamber. Open symbols: in the absence of nitrogen. Filled symbols: nitrogen present.

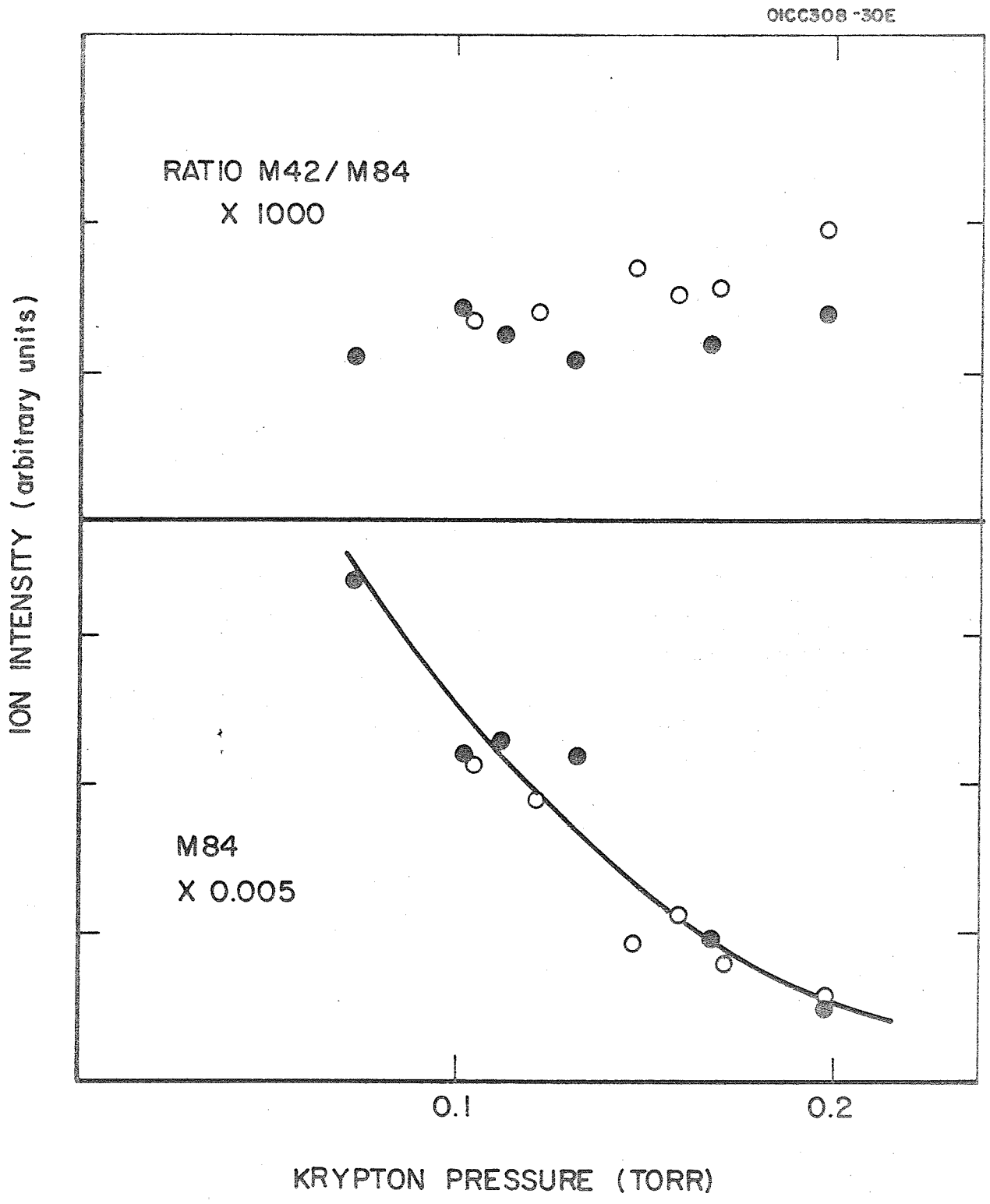

Figure 16. Krypton Ion Signals and M42/M84 Signal Ratios as Function of Krypton Pressure in the Charge Transfer Chamber. Same Scale & Symbols as in Figure 15.

is formed in the gap region
nitrogen escaping through the ion entrance orifice, and that a portion of these N_2^+ ions re-enter the charge transfer chamber.

The experimental data indicate that the formation of N_2^+ by doubly charged krypton ions is not significant. This aspect will be discussed next. Figure 16 shows that by increasing the krypton pressure in the charge transfer chamber both the intensities of Kr^+ and Kr^{++} decrease in the same manner. The decrease of primary ion intensity with pressure has already been explained and is due to the combined effects of charge repulsion and lateral diffusion of ions traversing the charge transfer chamber. The covariance of Kr^{++} and Kr^+ ion intensities indicates that the reaction

$$(7) \qquad Kr^{++} + Kr \rightarrow Kr^+ + Kr^+$$

is not significant and this conclusion agrees with previous data (Ref.1). Consequently, if N_2^+ were produced mainly by charge transfer from Kr^{++} to nitrogen, the M28 ion intensity should increase with pressure similar to that of M32 due to charge transfer from Kr^+ to oxygen. Since the M28 ion intensity does not increase with pressure, it is concluded that doubly charged krypton ions cannot be the major precursor. Additional evidence for this conclusion is provided by the data in Table 5. It was found that by lowering the dc potential on the pusher electrode of the discharge (see Figure 1) the contribution of Kr^{++} ions to the total ion intensity could be diminished also. Table 5 shows relative ion intensities for pusher potentials of zero and 125 volts, and the signal ratios observed for the two experimental conditions. On a relative scale the Kr^{++} ion intensity at mass number 42 decreased by a factor of 16 when the pusher voltage is reduced to zero while the N_2^+ ion intensity decreases only by a factor of 1.6. On this basis not more than 33 percent of the M28 ion intensity can be due to N_2^+ formed by charge transfer involving doubly charged krypton ions.

Further experiments established that, quite generally, the primary ion source operating conditions were significant in determining the extent of N_2^+ formation. Relevant parameters are the discharge pressure and the involved electric fields. Ion intensities observed for various primary source operating conditions (while keeping other parameters constant) are compiled in Table 6. One set of data shows that increasing the pressure in the discharge decreases the amount of N_2^+ production relative to O_2^+ formation which may here serve as a standard. The other set of results shows again that a dc field in the discharge tube enhances N_2^+ production when an ion preaccelerating field is applied to the differentially pumped gap region, but it shows also that in the absence of a preaccelerating field the application of a pusher potential decreases the relative N_2^+ contribution. These observations indicate that two effects are important: one occurs in the absence of any dc fields. Then the ions are extracted from the discharge solely by the flow of plasma (i.e., ions plus electrons) through the exit orifice and the discharge region must penetrate partially into the differentially pumped gap region. Under these conditions N_2^+

TABLE 5

VARIATION OF PRIMARY AND SECONDARY ION INTENSITIES (ARBITRARY UNITS) WITH DISCHARGE SOURCE PUSHER VOLTAGE (PV). PREACCELERATING VOLTAGE 150, CHARGE TRANSFER CHAMBER PRESSURE 104 MICRONS.

Mass Number	PV = 0	PV = 125	Intensity Direct	Ratio Normalized
85	36	49	0.73	1.00
84	13500	17800	0.76	1.04
42	10	195	0.05	0.07
29	152	208	0.73	1.00
28	35	71	0.49	0.67
32	56	70	0.80	1.10

TABLE 6

SECONDARY ION INTENSITIES FOR VARIOUS PRIMARY SOURCE CONDITIONS

Discharge Pressure		Low	Medium	High	High	High	High	High	Low
Charge transfer Chamber Pressure (microns)		170	170	170	120	120	120	120	120
Preaccelerating Voltage		0	0	0	150	150	0	0	0
Discharge Pusher Voltage		0	0	0	0	125	125	0	0
ion intensities (arbitrary units)	M28	17	2	0.5	3.5	15	12	2.5	32
	M29	4	8	8	41	52	43	7	4
	M30	7	45	33	2	2.5	2.0	34	12
	M32	32	18	9	89	110	107	9	20
Signal Ratio M28/M32		0.53	0.11	0.05	0.04	0.13	0.11	0.29	1.6

formation can be due only to an interaction of nitrogen with the discharge. In the presence of dc fields, ions are extracted efficiently while electrons are held back so that the plasma penetration is curtailed. The source of nitrogen ionization due to the plasma penetration is then removed. On the other hand, the imposition of a dc electric field on the microwave discharge as well as the lowering of discharge pressure increase the average energy acquired by the electrons in the discharge, so that the formation of excited ions and doubly charged ions is enhanced. Thus, it appears that at least some of the observed nitrogen ionization is caused by metastable excited krypton ions. Their contribution to the total ion population would depend critically on the discharge operating parameters. A low population of excited ions would be achieved with high discharge pressures and low electric fields.

It is also significant to note from the data in Table 6 that the application of an electric field in the gap region in addition to the fields existing in the discharge does not increase the N_2^+ generation. Instead a decrease is observed relative to O_2^+ formation. Accordingly, the acclleration of ions to kinetic energies exceeding that required for nitrogen ionization is not the major factor responsible for N_2^+ formation. Evidently, the fast ions are quickly thermalized by collisions in the charge transfer chamber.

From the sum of these data it is concluded that the residual ionization of nitrogen has two causes: (a) residual interaction with the boundary of the primary ion source, and (b) ions with internal energy, probably produced in the discharge by energetic electrons. The first source of nitrogen ionization occurs in the differentially pumped gap and may be reduced further by a more efficient differential pumping system than has been available in the present experiments. Since the N_2^+ ions from this source enter the charge transfer chamber together with the other primary ions, the corresponding M28 signal should decrease as the buffer gas pressure in the chamber is increased.

The second source of nitrogen ionization occurs in the charge transfer chamber and is proportional to the contribution of the excited Kr^+ ions to the total primary ion intensity. Unless the excited ions are rapidly deactivated by collision, the M28 signal corresponding to this source should increase with increasing buffer gas pressure. From the observation that the M28 ion intensity remains approximately constant as the pressure in the charge transfer chamber is varied it appears that both sources of N_2^+ contribute almost equally to the nitrogen ionization under the employed experimental conditions.

E. Application to the Detection of Carbon Monoxide

On the basis of the results presented in the preceding section the feasibility of measuring carbon monoxide in the presence of nitrogen can

now be evaluated. From the data presented in Figure 14 the sensitivity for nitrogen for the ion intensity on mass number 28 is found to be 3.3×10^{-11} amps/torr or about 1 percent of that of carbon monoxide. This ratio of sensitivies can be improved if more favorable operating conditions are chosen. Raising the pressure in the charge transfer chamber from 90 torr to 180 torr improves the CO sensitivity by a factor of two while leaving that of N_2 approximately unchanged. Reducing the dc field in the discharge to zero will further reduce the signal strength for nitrogen ions by a factor of three while reducing the total intensity only by 20 percent. Combining these factors provides a total improvement in the CO/N_2 sensitivity ratio by a factor of five, so that the signal ratio is given by

$$\frac{I(CO)}{I(N_2)} = 0.5 \times 10^3 \frac{P(CO)}{P(N_2)}$$

The ratio of pressures which just doubles the signal observed on mass number 28 thus is $P(CO)/P(N_2) = 2 \times 10^{-3}$ or 2 parts per thousand of carbon monoxide in nitrogen. By a comparison with pure nitrogen a concentration of 0.5 parts per thousand carbon monoxide can probably be observed. These figures show that the discrimination between carbon monoxide and nitrogen achieved at the present stage of development of the charge transfer mass spectrometer technique is not yet sufficient to be useful for the measurement of trace amounts of CO in the human environment. At least a ten-fold better discrimination is necessary to reach the CO toxicity limit, and for a detection limit of 1 ppm an improvement by a factor of five hundred is required. To achieve this degree of improvement it is necessary to improve not only the differential pumping efficiency in the gap region, but also the ion source characteristics if krypton ions are to remain the principal primary ions.

V. CONCLUSIONS

The principal aim of the present investigation of charge transfer mass spectrometry was to separate the charge transfer chamber and the primary ion source by the interposition of a differentially pumped gap so that the interaction of the sample gas with the primary ion source is eliminated. The results obtained with this modified ion source arrangement indicate that the ionization of sample gas by a direct interaction with the primary ion source is greatly reduced, in accordance with expectation. Because the gap installation was made by modifying existing apparatus, the pumping efficiency available was not optimized and some residual interaction of sample gas with the fringes of the discharge in the gap region had to be tolerated. This unwanted type of ionization no longer had any effect upon the type of charge transfer mass spectra observed, but it resulted in a residual ionization of nitrogen, which covers the mass number 28 peak and interferes with the detection of CO. In addition, it was found that an ionic species generated in the discharge, probably metastable excited krypton ions contributes to the ionization of nitrogen. The mass spectrometric sensitivity of the charge transfer method for carbon monoxide was found to be about an order of magnitude less than expected. These factors preclude the descrimination of less than 5×10^{-4} parts of CO in nitrogen as the present stage of development. If krypton ions are retained as the major primary type of ions for the measurement of CO, a mode of operation of the discharge primary source or another type of ion source will have to be found which minimizes the generation of electronically excited, metastable krypton ions. For the study of hydrocarbons it appears from the few examples investigated that primary ions having an average recombination energy lower than that of krypton ions would be preferable on account of the reduced fragmentation expected to occur in the charge transfer mass spectra of such compounds.

REFERENCES

1. Satkiewicz, F. G., J. A. Myer, P. Warneck,"Techniques applicable to Mass Spectrometry of Gaseous Trace Contaminants," GCA Technical Report No. 69-4-N, Interim Report on Contract No. NAS12-641 (May 1969).

2. Warneck, P., J. N. Driscoll, C. Matthews, "Study of the Application of a Photoionization Mass Spectrometer to Analysis of Contaminant Gases," GCA Technical Report No. 69-10-N, Final Report on Contract No. NAS1-7794 (November 1969).

3. Gifford, A. P., S. M. Rock, D. J. Comaford, "Mass Spectrometer Analysis of Alcohols and other Oxygenated Derivatives," Anal. Chem. 21 1026 (1949).

4. Kuentzel, L. E., "Index of Mass Spectral Data," ASTM Special Publication No. 356, American Society of Testing & Materials, Philadelphia, Pa. (1963).

5. Fite, W. L., Phys. Rev. 89, 411 (1953).

6. Warneck, P., "Laboratory Measurements of Photodetachment Cross Sections of Selected Negative Ions," GCA Technical Report No. 69-13-N, Final Report under Contract No. NAS5-11157 (November 1969)

7. Ferguson, E. E., "Negative Ion-Molecule Reactions," Can. J. Chem.